

An Update on SURFRAD—The GCOS Surface Radiation Budget Network for the Continental United States

JOHN A. AUGUSTINE

Surface Radiation Research, NOAA/Air Resources Laboratory, Boulder, Colorado

GARY B. HODGES

Cooperative Institute for Research in the Environmental Sciences, University of Colorado, and Surface Radiation Research, NOAA/Air Resources Laboratory, Boulder, Colorado

CHRISTOPHER R. CORNWALL, JOSEPH J. MICHALSKY, AND CARLOS I. MEDINA

Surface Radiation Research, NOAA/Air Resources Laboratory, Boulder, Colorado

(Manuscript received 29 November 2004, in final form 18 April 2005)

ABSTRACT

The Surface Radiation budget (SURFRAD) network was developed for the United States in the middle 1990s in response to a growing need for more sophisticated in situ surface radiation measurements to support satellite system validation; numerical model verification; and modern climate, weather, and hydrology research applications. Operational data collection began in 1995 with four stations; two stations were added in 1998. Since its formal introduction to the research community in 2000, several additions and improvements have been made to the network's products and infrastructure. To better represent the climate types of the United States, a seventh SURFRAD station was installed near Sioux Falls, South Dakota, in June 2003. In 2001, the instrument used for the diffuse solar measurement was replaced with a type of pyranometer that does not have a bias associated with infrared radiative cooling of its receiving surface. Subsequently, biased diffuse solar data from 1996 to 2001 were corrected using a generally accepted method. Other improvements include the implementation of a clear-sky diagnostic algorithm and associated products, better continuity in the ultraviolet-B (UVB) data record, a reduced potential for error in the downwelling infrared measurements, and development of an aerosol optical depth algorithm. Of these, only the aerosol optical depth product has yet to be finalized. All SURFRAD stations are members of the international Baseline Surface Radiation Network (BSRN). Data are submitted regularly in monthly segments to the BSRN archive in Zurich, Switzerland. Through this affiliation, the SURFRAD network became an official part of the Global Climate Observing System (GCOS) in April 2004.

1. Introduction

The National Oceanic and Atmospheric Administration's (NOAA) Surface Radiation budget (SURFRAD) network is the first and only U.S. national-scale network to measure the surface radiation budget in a continuous mode. The present network consists of seven stations (Fig. 1). Monitoring began in 1995 with four stations; two were added in 1998, and the latest

station was installed in 2003. Owing to the quality, utility, and continuity of its datasets, SURFRAD has garnered a diverse and extensive clientele that includes the NOAA National Environmental Satellite, Data, and Information Service (NESDIS), the National Centers for Environmental Prediction (NCEP), the National Aeronautics and Space Administration (NASA), the United States Geological Survey (USGS), the European Centre for Medium-Range Weather Forecasts (ECMWF), academia, state governments, and private industry. In April 2004, SURFRAD became an official part of the Global Climate Observing System (GCOS) through its affiliation with the international Baseline Surface Radiation Network (BSRN). The purpose of

Corresponding author address: John A. Augustine, NOAA/Air Resources Laboratory, R/ARL, 325 Broadway, Boulder, CO 80305.

E-mail: John.A.Augustine@noaa.gov

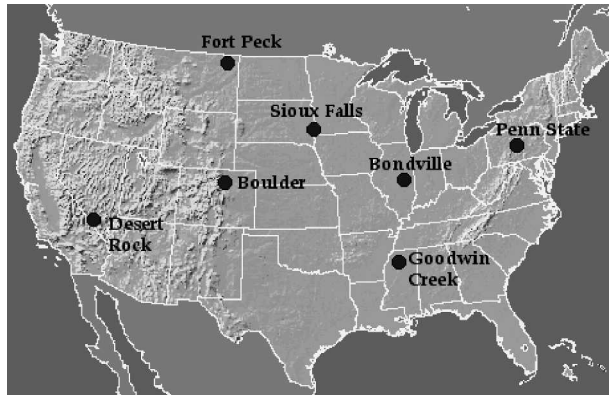


FIG. 1. The SURFRAD surface radiation budget network.

this article is to provide an update on the status of the SURFRAD network since it was first documented in Augustine et al. (2000).

2. Background

The four quantities that compose the surface radiation budget are the upward and downward components of solar and thermal infrared irradiance. Each of these parameters is measured independently at SURFRAD stations. Other radiation measurements include ultraviolet B (UVB), photosynthetically active radiation (PAR), and spectral solar irradiance for aerosol optical depth (AOD) calculations. Irradiance measurements are supplemented with a meteorological suite that includes station pressure, wind speed, wind direction, air temperature, and relative humidity. In compliance with accepted climate monitoring practices, all radiometers, except the MFRSR, are replaced annually with freshly calibrated units, and the instruments that are removed are compared to their replacements by means of an overlap method described in Augustine et al. (2000).

SURFRAD's broadband solar radiometers have been calibrated at the Department of Energy's (DOE) National Renewable Energy Laboratory (NREL). Their cavity radiometers have calibrations that are traceable to the World Radiation Reference (WRR), which is a collection of seven absolute cavity radiometers maintained by the World Radiation Center in Davos, Switzerland. Beginning in 2005, SURFRAD's broadband solar instruments will be calibrated by the World Meteorological Organization's (WMO) Region-4 Regional Solar Calibration Center¹ at NOAA in

¹ Operated by NOAA's Climate Monitoring and Diagnostics Laboratory, soon to be part of the new NOAA Earth System Research Laboratory's Global Monitoring Division.

Boulder, Colorado, whose absolute cavity radiometers also have traceability to the WRR.

A world standard for calibration of broadband thermal infrared instruments has not yet been identified. However, the three standard pyrgeometers that are used to calibrate SURFRAD monitoring pyrgeometers are sent for calibration annually to the World Radiation Center's Physikalisch-Meteorologisches Observatorium (PMOD) in Davos, Switzerland. The PMOD blackbody infrared radiation calibration unit was chosen because it performed well in a round-robin test that involved a blind comparison of several such devices (Philipona et al. 1998). After the SURFRAD standard pyrgeometers are calibrated in the blackbody, their calibrations are fine tuned by running them outdoors against PMOD's reference group of four pyrgeometers, which are referred to as the World Pyrgeometer Standard Group. That group is traceable to the Absolute Sky-Scanning Radiometer (ASR; Philipona 2001), which was used as a reference in two international pyrgeometer comparisons, IPASRC-I (Philipona et al. 2001) and IPASRC-II (Marty et al. 2003).

Daily SURFRAD data files from each station are checked and published on a quasi-daily basis to an ftp site online at <ftp://ftp.srrb.noaa.gov/pub/data/surfrad/>. To ease data access and to protect the user's privacy, no fee or registration is required. SURFRAD data are periodically reprocessed when improvements are implemented or when problems are discovered. After any reprocessing exercise, a short notice is placed on the SURFRAD Web page to inform data users. In addition to the notice, the purpose for the reprocessing, the date that the data were reprocessed, and the stations and period affected are cataloged on the "problems" link of that page. For details on the network's operating practices, measurement accuracies, quality assurance, etc., see Augustine et al. (2000).

3. The growing need for surface radiation and energy flux measurements

Traditional climate measurements such as temperature and precipitation describe the atmosphere's lagged response to climate change, but they convey little as to its cause. Mechanisms of climate change, such as a long-term increase or decrease in cloud cover, persistent changes in the concentrations of greenhouse gases, or systematic changes in aerosol loading may be more readily reflected in the character of the surface radiation budget and surface heat fluxes. It follows that monitoring the surface energy budget over the long term could offer a gauge to the near-term evolution of the earth's climate.

Well-calibrated and well-maintained ground stations provide the necessary validation that is critical to the success of climate modeling and satellite-based efforts to assess the surface radiation and energy budgets on the global scale. A National Academy of Sciences' Committee report on Global Change Research (CGCR 1998) echoed this need by stating that sustained surface observations provide continuity to the climate record, as well as the truth needed for verifying satellite systems and environmental models. Recent attempts to assess the global surface radiation budget have been incorporated into NASA's Earth Observing System (EOS) research satellites, which are the testbeds for NOAA's next generation operational environmental satellite, the National Polar-Orbiting Operational Environmental Satellite System (NPOESS). The sophisticated monitoring packages of three EOS satellites include the Clouds and the Earth's Radiant Energy System (CERES) instrument that is designed to estimate the surface radiation budget, and the Moderate Resolution Imaging Spectroradiometer (MODIS) that estimates surface albedo and aerosol optical depth. SURFRAD datasets are routinely used to validate EOS products (e.g., Jin et al. 2003), as well as NESDIS surface radiation products derived from Geostationary Operational Environmental Satellite (GOES) data (Sun and Pinker 2003; Pinker et al. 2003). Likewise, in lieu of parameterizations, many of the newest weather and climate models compute surface radiation and heat fluxes explicitly, and also include the effects of clouds and aerosols. The developers of these complicated algorithms depend on the unique validation datasets provided by SURFRAD, other BSRN stations, and DOE's Atmospheric Radiation Measurement (ARM) Program (Morcrette 2002a,b).

4. Recent additions and improvements to the SURFRAD network

a. New station installed in 2003

In cooperation with the USGS, a seventh SURFRAD station (Fig. 2) was established in June of 2003 near the Earth Resources Observation Systems (EROS) Data Center. It is located about 24 km north of Sioux Falls, South Dakota, at 43.73°N, 96.62°W, and 473 MSL. Other surface observations collocated with the new SURFRAD station are a GPS water vapor retrieval station (Wolfe and Gutman 2000) and a Climate Reference Network (CRN) station (Heim 2001). The nearest operational National Weather Service (NWS) rawinsonde site is at Aberdeen, South Dakota, about 200 km northwest of Sioux Falls. As with the other SURFRAD stations, rawinsonde soundings for 0000



FIG. 2. The newest SURFRAD station near Sioux Falls, SD. The spherical structure in the background houses the EROS Data Center's Landsat antenna. All SURFRAD stations have been improved and reconfigured to the model shown. New solar trackers have been installed, the pyrgeometer that measures downwelling thermal infrared irradiance has been moved from the main platform to the solar tracker shade platform, and the pyranometer that measures diffuse solar irradiance has been changed from a solid-black sensor pyranometer to an Eppley model 8-48.

and 1200 UTC are interpolated to the location of the new station on a daily basis. The interpolated soundings, which are made available from the SURFRAD Web page, are useful for initializing radiative transfer models and for computing column water vapor.

b. Downwelling thermal infrared measurement improved

During the instrument exchanges in 2000, the pyrgeometer that measures downwelling thermal infrared irradiance was moved from the main platform to the shade platform of the solar tracker. Throughout the daytime, a shade ball casts a shadow on the dome that covers the thermopile sensor of the pyrgeometer. Shading the pyrgeometer sensor minimizes errors associated with inward infrared emission from the dome to the thermopile. That emission contributes a superfluous signal to the thermopile that must be removed. A method to correct for the dome emission was developed by Albrecht and Cox (1977) and is employed by SURFRAD. That method is accurate if the measured dome temperature, from which the dome emission is computed, is representative of the entire dome—that is, if there is no temperature gradient across the dome. Shading the pyrgeometer dome ensures that the sun's beam does not preferentially heat the dome's sunward side, causing a skewed dome temperature distribution and resultant errors. The practice of shading the pyrgeometer dome complies with the standards of operation recommended by the BSRN (McArthur 1998).

c. Diffuse solar measurement improved

Solid-black thermopile sensor pyranometers that were first used for the diffuse solar measurement in SURFRAD were replaced with Eppley model 8–48 pyranometers during the 2001 instrument exchanges. This change was necessary because the solid black thermopile sensors have an inherent problem caused by radiational (infrared) cooling of the sensor's surface (Dutton et al. 2001; Gulbrandsen 1978). This cooling is capable of producing erroneous negative signals of up to -30 W m^{-2} under dry, clear-sky conditions. These errors are obvious at night when there is no solar signal, but are also present in the daytime global and diffuse solar measurements. The advantage of the model 8–48 pyranometer is that its thermopile signal results from a differential between separate black (hot junction) and white (cold junction) surfaces that make up the receiving area of its sensor. Those surfaces absorb solar radiation differently, as designed, but radiate equally in the thermal infrared. Thus, infrared cooling of the 8–48's sensor surface produces no differential signal, and consequently, no erroneous offset. The model 8–48 pyranometer is not used for global solar measurements because of the instrument's known variable response with regard to diurnal changes in the incident angle of the solar beam. Such dependencies associated with the solar beam are not an issue when the sensor is shaded for the diffuse solar measurement.

It has long been recognized that the best measure of total solar irradiance on a horizontal surface is the algebraic combination of the direct normal and diffuse components:

$$\text{Total solar irradiance} = \text{direct}(\cos[\text{SZA}]) + \text{diffuse}, \quad (1)$$

where SZA is the solar zenith angle. Multiplying the measured direct normal irradiance by the cosine of the SZA yields the horizontal component of the solar beam. Of the solar radiation measurements in SURFRAD, direct normal solar has the highest accuracy (typically $\pm 2\%$ – 3%). The pyrheliometers used for that measurement are characteristically stable because 1) they are continually trained on the sun and thus do not have problems related to changes in the sun's incident angle, and 2) they are calibrated directly with an absolute cavity radiometer whose calibration is traceable to the World Radiation Reference. Thus, by improving the accuracy of the diffuse solar measurement by changing to the Eppley 8–48, the accuracy of the total solar irradiance calculation has been improved. The global solar measurement made with a single pyranometer at SURFRAD stations is now considered sec-

ondary to the component sum, and is reported only for redundancy and data quality control. The component sum total solar irradiance is not included in SURFRAD data files, but the solar zenith angle is listed for each reporting time, which makes component sum calculation straightforward for users.

d. Historical SURFRAD diffuse measurements corrected

A way to correct erroneous daytime offsets in diffuse measurements made with solid-black sensor pyranometers has been developed by Dutton et al. (2001) for situations where a pyrgeometer is also present. A relationship is established between the offset of the diffuse pyranometer and the collocated pyrgeometer's thermopile signal using nighttime data, when the diffuse offset errors are obvious. The pyrgeometer thermopile signal is used as a proxy for the thermal infrared cooling of the pyranometer's sensor. That relationship is then applied to correct daytime data. Because this method is measurement based, unique correction relationships must be developed for each distinct pyranometer/pyrgeometer pair that has been deployed.

The method reported in Dutton et al. (2001) was developed using data from collocated Eppley Precision Spectral Pyranometers (PSP) and Eppley Precision Infrared Pyrgeometers, which share the same thermopile configuration in their sensors. Although the Spectrolab pyranometers² used in SURFRAD and Eppley PSPs both have solid-black-sensors, the two instruments differ slightly in design. The thermopile in the Spectrolab pyranometer is in direct contact with a mass of solid metal that fills the interior of the instrument, whereas the thermopile of the Eppley PSP is suspended above a void in the instrument body. Experience from operating Spectrolab and Eppley PSPs side-by-side at NOAA's Table Mountain Test Facility near Boulder, Colorado, has shown that the average nighttime offset of the Spectrolab pyranometer is consistently about half of that associated with an Eppley PSP. Owing to this difference, the Dutton et al. (2001) method was adapted, but not applied directly to diffuse measurements made with Spectrolab pyranometers.

Periods of deployment for all unique diffuse-pyranometer/pyrgeometer pairs used in the SURFRAD network were identified and nighttime data were plotted as prescribed by Dutton et al. (2001). A sample plot representing 14 months for Desert Rock, Nevada, is shown in Fig. 3. The ordinate represents the

² Manufactured in the 1970s by Spectrolab Solar Power Systems of Sylmar, California.

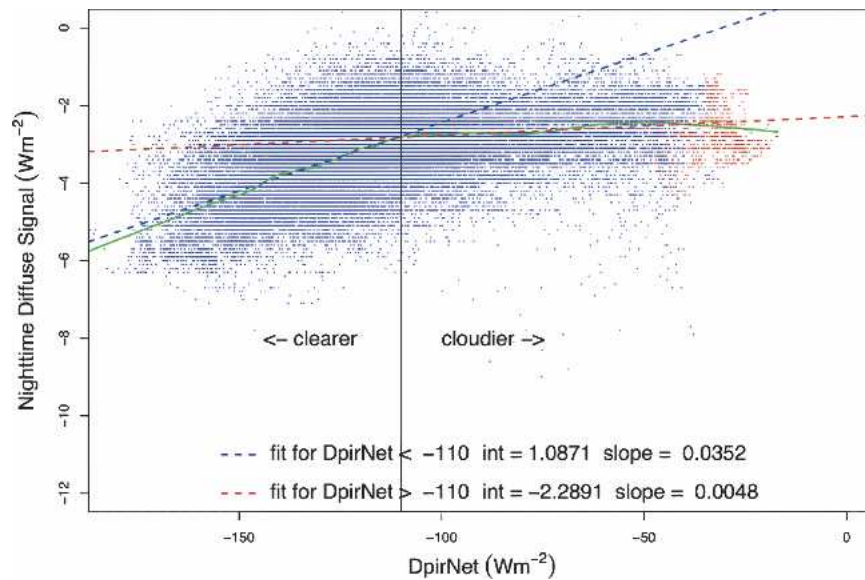


FIG. 3. Nighttime signals from a diffuse-measuring Spectrolab pyranometer vs the thermopile signal of a collocated pyrgeometer converted to W m^{-2} (referred to as DpirNet). Data are from Desert Rock, NV, and represent the period 15 Mar 1998–22 May 1999. Red points represent nearly or fully saturated conditions, and blue points represent all other conditions. The green line is a locally weighted robust best fit (LOESS) to all of the data. The blue dashed line is a least squares linear fit to the data to the left of the inflection point in the LOESS fit, and the red dashed line is a least squares linear fit to the points to the right of the inflection point.

nighttime diffuse pyranometer offset converted to watts per square meter. Note that the range of the nighttime diffuse data is entirely negative, indicating the signal was produced by radiational cooling of the pyranometer's solid black sensor. The abscissa in Fig. 3 represents the thermopile signal of the collocated pyrgeometer converted to watts per square meter. Pyrgeometer thermopile output is referred to as "DpirNet" in Dutton et al. (2001), and that same nomenclature is used in Fig. 3 as well as in the following discussion. Generally, the more negative the DpirNet value, the clearer the sky conditions.

Red dots on the right portion of Fig. 3 represent periods when the atmosphere is saturated, or nearly so; blue dots represent all other times. The green line is a LOESS "locally weighted" best fit (Cleveland 1979; Cleveland and Devlin 1988) to the plotted data. The LOESS fit shows two distinct linear regimes on either side of an inflection point at a DpirNet value of -110 W m^{-2} . A larger slope occurs to the left of the inflection point on the "clear-sky" side of the plot. The dashed blue line is the least squares linear fit to those data and is used to correct diffuse measurements associated with DpirNet values less than -110 W m^{-2} . On the more moist and cloudy right side, the LOESS fit slope is smaller. The dashed red line is the least squares

linear fit to those data and is used to correct diffuse data associated with the range of DpirNet values on that side of the plot. Whether the air was saturated (red points) appears to be irrelevant to the relationship. This dual-linear regime is characteristic of all SURFRAD stations regardless of climate, although the scatter and position of the inflection point varied slightly. The method applied by Dutton et al. (2001) did not consider the dual-regime nature of these plots. They computed one linear fit to all of the data that was constrained to pass through the origin.

The appendix summarizes the diffuse solar correction plots for all of the unique pyranometer/pyrgeometer pairings at the six SURFRAD stations between 1995 and 2000. Forty-nine plots of the type shown in Fig. 3 were produced. Forty showed the dual-linear structure described above. The appendix lists the DpirNet values associated with the inflection points for each of those plots; the mean is $-100 \text{ W m}^{-2} \pm 10$. Uncertainties of the diffuse corrections at 95% confidence, generally less than $\pm 2 \text{ W m}^{-2}$, are also listed. One period during 1997 at Table Mountain has an abnormally low inflection point DpirNet value of -150 W m^{-2} . A malfunctioning fan in the pyrgeometer ventilator heated the instrument, which led to a greater degree of radiational cooling of the pyrgeometer sensor, and

thus higher than normal DpirNet values. However, that abnormality had no ill effect on the diffuse correction.

Figure 3-type plots for nine of the instrument-pair epochs showed no coherent tendencies. Thus, the diffuse solar data in those periods could not be corrected in the same manner as the others. Rather than make no corrections, the pyrgeometer data were disregarded and the daytime diffuse correction for individual daytime periods within those nine epochs was simply defined as the mean diffuse offset from the previous night. This correction method is commonly used when pyrgeometer data are not available.

In March 2004 the entire SURFRAD dataset prior to the deployment of the Eppley 8–48 pyranometers was reprocessed to correct the historical diffuse solar data. Corrected diffuse solar values replaced the biased values in the SURFRAD data files. To be consistent, the bimodal correction analysis was also applied to the few epochs when an Eppley PSP was used for the diffuse solar measurement.

e. Improved surface net solar calculation

Net solar, net thermal infrared, and total net radiation are reported in the SURFRAD data files. Total surface net radiation is generally defined as the sum of net solar and the net infrared:

$$\begin{aligned} \text{Total surface net radiation} = & (\text{Solar down} - \text{Solar up}) \\ & + (\text{Infrared down} \\ & - \text{Infrared up}). \end{aligned} \quad (2)$$

At SURFRAD stations, “Solar up,” “Infrared up,” and “Infrared down” are each measured by single radiometers. “Solar down” is measured in two ways, as the component sum of separate direct-normal and diffuse solar measurements, and by a single pyranometer. If the component sum cannot be computed, the less accurate global solar measurement from the single pyranometer is used for “Solar down.”

The net solar calculation has been improved in two ways. The addition of the diffuse solar measurement in 1996 made the more accurate component sum possible for “Solar down.” Accuracy of the component sum was improved in 2001 with the introduction of the Eppley 8–48 pyranometer for the diffuse measurement. Historical corrections to the diffuse solar data, discussed in the previous section, likewise improved the net solar calculation for the period before the Eppley model 8–48 pyranometer was used. The second improvement involved the extension of the net solar calculation beyond sunset to the end of civil twilight. In the original SURFRAD processing code, surface net solar was

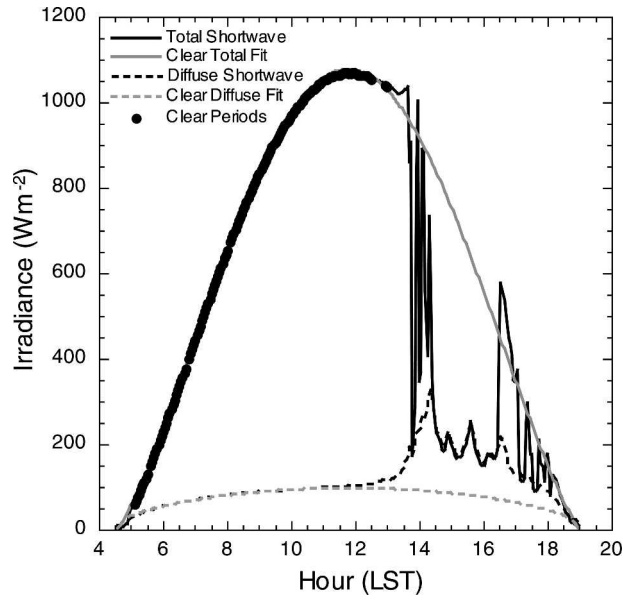


FIG. 4. Measured total solar (solid black) and diffuse (dashed black) irradiance, and clear-sky envelopes (gray) for those parameters for the Table Mountain SURFRAD station on 21 Jun 2004. Black dots indicate times determined to be cloud free by the Long and Ackerman (2000) clear-sky identification algorithm.

computed only for times when the sun was either at or above the horizon. However, downwelling solar radiation is finite in the diffuse during civil twilight, when the solar zenith angle is between 90° and 96° . In February 2004, the full SURFRAD data record was reprocessed to include these improvements.

f. Clear-sky identification analysis applied to SURFRAD data

An automated clear-sky identification algorithm (Long and Ackerman 2000) has been adapted to SURFRAD data. The algorithm operates on one day of solar component data, and uses empirical methods to objectively determine periods of totally clear skies, at the temporal resolution of the data. The method employs tests based on the premise that cloud-free skies exhibit different characteristics than cloudy or hazy skies in the components of downwelling solar irradiance. Identified clear-sky periods correspond to conditions of totally cloud-free skies for an effective 160° field of view centered on the local zenith. In the example shown in Fig. 4, the solid dots represent the 3-min periods that were determined to be cloud free.

If enough clear periods are identified in a particular day, an empirical fit is applied to only the clear-sky irradiance values. The result is an analytical expression that provides a best estimate of the clear-sky irradiance

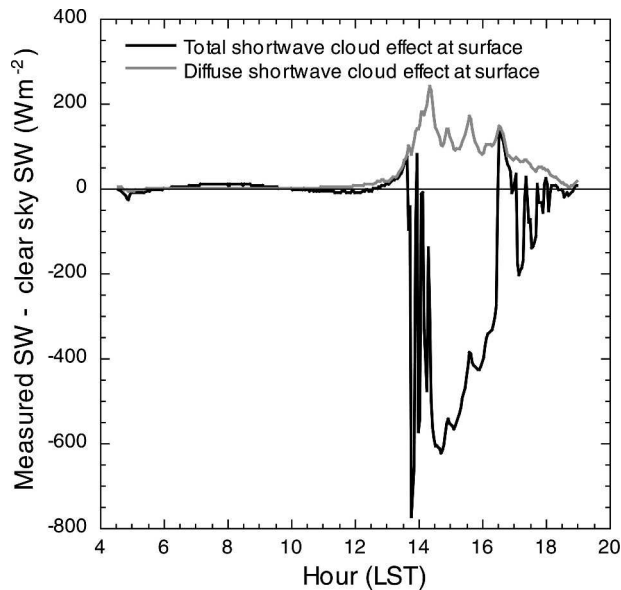


FIG. 5. Time series of the effect of clouds on surface shortwave radiation at the Table Mountain SURFRAD station for 21 Jun 2004. The black solid curve is the difference between measured and clear-sky total solar in Fig. 4, and the gray curve is the difference between measured and clear-sky diffuse in Fig. 4.

envelope for the entire daylight period. Separate fits are made for global solar, the component sum, diffuse solar, ultraviolet-B, photosynthetically active radiation, and other parameters. Obviously, not every day would have enough clear periods to support meaningful diurnal clear-sky fit. For those days the algorithm interpolates the coefficients of the clear-sky fit equations from the closest days before and after when fits were possible, thus achieving a continuum of daily clear-sky envelopes for the entirety of the record. Examples of clear-sky fit envelopes for total and diffuse solar irradiance are shown as gray curves in Fig. 4. Note in Fig. 4 that during the afternoon of 21 June 2004, clouds generally increase the measured diffuse and reduce the total solar irradiance from that which would be expected under clear skies (cf. the gray and black curves). However, on the fringes of the cloudy period, near 1300 and 1700 LST, the clouds act to briefly increase the total solar irradiance at the surface to levels higher than the clear-sky values. The difference between the measured and clear-sky irradiance provides a quantitative estimate of the radiative effect of the clouds on the surface (Fig. 5). Because the clear-sky identification is measurement based, these quantitative cloud effects have the same error as the original measurements. Other products of the clear-sky analysis are unique data quality control parameters and an empirically derived hemispheric cloud fraction product (Long et al. 1999).

The clear-sky identification code has been applied to all historical SURFRAD data, and is run for new data on a quasi-monthly basis. These products are organized into daily files for each station and are distributed by anonymous ftp.

g. Aerosol optical depth algorithm developed

The Multifilter Rotating Shadowband Radiometer (MFRSR) deployed at SURFRAD stations is a passive spectral instrument that alternately measures global and diffuse irradiance in six narrowband channels of the solar spectrum near 415, 500, 615, 670, 870, and 940 nm. MFRSR data may be processed to mimic the measurements from a sunphotometer and thus can be analyzed for aerosol optical depth. The MFRSR is typically not calibrated for absolute irradiance, but rather, it is usually calibrated in a relative sense using the Langley method (Shaw 1983). A Langley calibration should use only pristine and unimpeded direct-normal narrowband measurements of the solar beam. The selection of such unobstructed measurements from an MFRSR time series can be labor intensive because the instrument is unattended and its data include all weather conditions. For SURFRAD, Langley calibration data are selected by cross referencing MFRSR measurement times with periods identified as completely cloud free by the Long and Ackerman (2000) clear-sky analysis. This novel method was successfully applied to calibrate the MFRSR 500-nm channel in Augustine et al. (2003).

Advances achieved since Augustine et al. (2003) clear the way for an aerosol optical depth product for SURFRAD. They include

- 1) interpolation of periodic Langley calibrations and associated error to individual days;
- 2) expansion of the MFRSR calibration and optical depth analysis to all channels of the MFRSR, except 940 nm, which is designed for precipitable water retrievals;
- 3) better-resolved molecular scattering calculations using the measured station pressure;
- 4) automated Web access of daily total ozone over station locations for more accurate quantification of ozone absorption in the MFRSR measurement bands;
- 5) implementation of a more common “propagation of error” analysis to the aerosol optical depth product; and
- 6) application of a cloud-screening algorithm for daily aerosol optical depth time series.

Periodic Langley channel calibration values are normalized to the mean Earth–Sun distance so that their calibrations can be analyzed for drift and interpolated

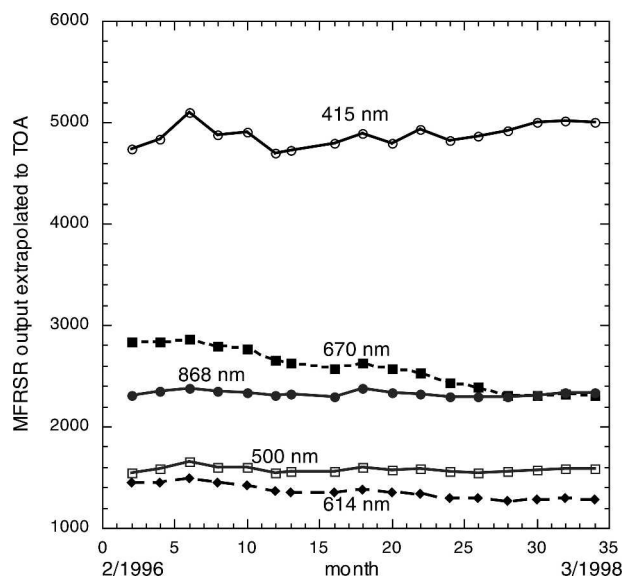


FIG. 6. Time series of calibration values in counts for five channels of the Multifilter Rotating Shadowband Radiometer deployed at the Bondville SURFRAD station from Jan 1996 through Mar 1998.

to individual days. Figure 6 shows time series of normalized MFRSR channel calibration values for Bondville, Illinois, between January 1996 and April 1998. Linear equations fit to such time series are used to interpolate the channel calibrations to individual days within the time series. The interpolated normalized calibrations represent a circular orbit of the Earth, and are corrected back to the proper Earth–Sun distance before being applied. Errors in AOD associated with these Langley calibrations are estimated using a standard “propagation of error” analysis, as described in Michalsky et al. (2001). Linear trends are also fit to the errors, thereby allowing the uncertainty of the AOD retrievals to be interpolated to individual days. Because the Langley calibrations and errors are instrument specific, new calibration and error trends must be established when an MFRSR is replaced.

The SURFRAD AOD analysis program operates on 1 day of raw MFRSR spectral data. It first retrieves the channel-specific calibrations for that day from the appropriate calibration time series, and applies them to the measured voltages. The result is a daily time series of *total optical depth* for each channel. To extract *aerosol optical depth* from the total optical depth values, the effects of molecular scattering and ozone absorption must be removed. The contribution of molecular scattering is computed at the resolution of the data using the station pressure measured at the SURFRAD station. Ozone absorption is computed from daily total ozone values for each station’s location that are re-

trieved automatically from the Total Ozone Mapping Spectrometer (TOMS) Web site.

Aerosol optical depth can only be computed for times when the MFRSR has an unobstructed view of the sun. Because MFRSRs are unattended, daily time series of AOD must be screened for cloud contamination. Because aerosol optical depth values rarely exceed 1.0, all AOD values greater than 2.0 are removed to rid the time series of obvious cloud signals. The remaining data are subjected to a stability analysis where spikes caused by more subtle cloud contamination are removed from the relatively stable AOD signal. Although an algorithm for removing cloud contamination from the daily AOD time series has been developed, it needs to be rigorously tested. Also, the series of algorithms used for calibration, molecular scattering, ozone absorption, AOD analysis, and cloud screening needs to be implemented in a robust manner before a daily AOD product is finalized.

h. Improved UVB data

The basis for calibration of SURFRAD UVB broadband monitoring instruments is a set of three standard UVB broadband radiometers that are maintained at NOAA’s Central UV Calibration Facility (CUCF). The standards are calibrated by referencing them to a collection of highly accurate UV spectroradiometers that are occasionally operated together at the CUCF Field Test Facility at Table Mountain near Boulder, Colorado (Lantz et al. 1999). In that process, an absolute calibration for the three UVB broadband standard instruments is defined as a function of solar zenith angle. Over an 11-yr period, the standards’ collective calibration has changed by approximately 11% at a steady rate of about 1% per year.

Before a UVB instrument is deployed at a SURFRAD station, it is calibrated by operating it alongside the three standards. The ratio of the mean daily integrated output voltage of the standards to the daily integrated output voltage of the test instrument is the scale factor that relates the test instrument to the standards. UVB irradiance at a SURFRAD station is computed by multiplying the output voltage from the monitoring UVB instrument times its scale factor, and then times the standards’ calibration factor appropriate to the solar zenith angle at the time of the measurement.

In the past, the closest UVB standards’ calibration prior to the day being processed was used to convert the measured output voltage from a monitoring instrument to irradiance. This practice resulted in step changes in network UVB data whenever a new standards’ calibration was introduced. In early 2004, the

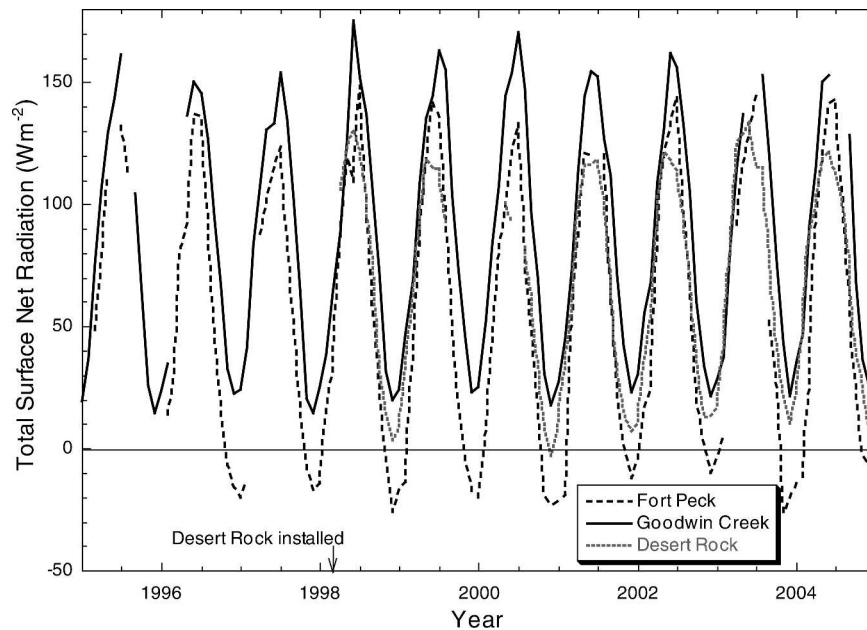


FIG. 7. Time series of mean monthly total surface net radiation at three SURFRAD stations. Fort Peck and Goodwin Creek are two of the original stations that began operations in 1995. The Desert Rock station was installed in Mar 1998. The year labels on the abscissa are positioned at Jan.

SURFRAD processing code was modified to linearly interpolate the standards' calibrations to the day being processed. This change eliminated step shifts in network UVB irradiance, and improved the accuracy of the network UVB data. In September 2004, the entire SURFRAD dataset was reprocessed to include this improvement.

5. Long-term time series from SURFRAD

Figure 7 presents a fundamental product from the SURFRAD network. It is a 10-yr time series of total surface net radiation monthly averages from two original stations and the Desert Rock station that was installed in March 1998. Gaps in the time series represent months when total surface net radiation could not be computed because one or more of the parameters that contribute to the surface radiation budget was missing for more than 30% of the month.

Total surface net radiation represents the amount of radiation absorbed at the surface of the earth that is available to evaporate water, heat the air, and heat the subsurface. Net solar is positive in the daytime and zero at night, and net infrared is almost always negative. Over the globe these terms balance, but generally they do not balance at individual locations. The primary factors that govern total surface net radiation are the incident angle of the incoming solar beam (which is gov-

erned by latitude and the time of year), the character of the surface, the skin temperature of the surface, atmospheric humidity, cloud cover, and aerosols.

The highest total surface net radiation occurs at the southern-most SURFRAD station, Goodwin Creek (34.25°N), and it never goes below zero (more radiation going out than coming in) during the coldest months. Several factors lead to these characteristics. Abundant atmospheric water vapor there limits the outgoing infrared. Owing to Goodwin Creek's low latitude, the incoming solar beam is more direct and thus more intense than at other SURFRAD stations. Also, it rarely snows there, minimizing the periods of great solar loss owing to intense reflection.

The northernmost station, Fort Peck (48.31°N), shows the greatest interannual variation of total surface net radiation among the stations shown, and it is the only station whose surface net radiation consistently goes below zero in the cold season. The variation in the magnitude of winter minima at Fort Peck may be largely governed by the persistence of snow cover. When snow covers the surface for several months, for example the winters of 1997 through 2001 and 2004, the high reflectance of the snow surface drastically reduces the surface net radiation. During winters when the snow cover is less persistent (e.g., 2002, 2003, and 2005), the seasonal minima of total surface net radiation are less negative. Karl et al. (1993) reports that interannual

variability and trends in snow cover over “seasonal temperature sensitive snow cover regions” of North America, which includes Montana, may have an important bearing on climate change.

Desert Rock (36.63°N), the driest station, has a fairly stable interannual variation of total surface net radiation. Owing to its sun-rich climate, Desert Rock achieves the greatest mean monthly surface *net solar* values (not shown) of any SURFRAD station. Ironically, however, it also has the lowest total surface net radiation during the warm season. That is possible because Desert Rock also has the greatest infrared losses of any station because of high surface skin temperatures, a general lack of cloud cover, and persistent low humidity.

6. Summary

NOAA initiated the nation’s first continental surface radiation budget network in the early 1990s to support new satellite systems; climate and weather modeling; and basic climate, weather, and hydrology research. Operational measurements began in 1995 with four stations. The network expanded to six stations in 1998. Since the initial documentation of SURFRAD (Augustine et al. 2000), several additions and improvements have been made. A seventh station was added near Sioux Falls, South Dakota, in June 2003. In compliance with measurement standards defined by the international BSRN, the pyrgeometer that measures downwelling thermal infrared radiation has been shaded to reduce the potential for errors associated with differential heating of its dome. Since 2001, the diffuse solar measurement has been made with an Eppley 8–48 pyranometer that does not have the offset problem characteristic of solid-black sensor pyranometers. All SURFRAD diffuse solar data from the period prior to the switch to the model 8–48 pyranometer were corrected using a generally accepted method that was adapted for application to SURFRAD’s Spectrolab pyranometers. Advances in data processing include the extension of the net solar calculation to civil twilight and better continuity in the UVB data across calibration changes. An algorithm that empirically derives daily clear-sky envelopes for many solar radiation parameters has been adapted to SURFRAD data, allowing for an accurate quantitative assessment of the radiative effect of clouds on the surface at the temporal resolution of the data. Information generated by the clear-sky algorithm was applied in a novel way to calibrate Multifilter Rotating Shadowband Radiometers at SURFRAD stations, which led to the development of an aerosol optical depth algorithm. However, an AOD

product has yet to be finalized. Finally, through its affiliation with the BSRN, SURFRAD became an official part of the Global Climate Observing System in April 2004.

7. Plans and possibilities

A constraint of the current SURFRAD clear-sky identification algorithm is that it operates only on solar data, and thus is limited to daytime. A prototype nighttime clear-sky identification algorithm has been developed at the Department of Energy’s ARM Program and is now being tested. With such a product, quantitative cloud effects on surface radiation may be computed for all hours of the day, thus making the clear-sky product more useful.

To better cover the climate zones of the United States, and to satisfy the expressed needs of NESDIS, the SURFRAD network should be expanded to include another desert site in southern New Mexico or Arizona, and a forested site in New England. Beyond these, three other possibilities for network expansion are the Pacific Northwest, the southeast United States, and south Texas, bringing the number of stations to 12. Global expansion may become a reality when the Global Monitoring Division of the Earth Systems Research Laboratory becomes part of the new organizational structure of NOAA Research in Boulder, Colorado.

As of 2004, only three SURFRAD stations have collocated sensible, latent, and soil heat-flux measurements. To further address the modern needs of the climate, weather, and hydrology modeling communities, surface heat flux stations should be installed at all SURFRAD stations, making it a true surface energy budget network that would better support the mission-critical needs of NOAA’s NCEP and NESDIS, as well as those of NASA.

Acknowledgments. The maintenance of the SURFRAD radiation budget network at a high level of quality is the result of the collective efforts of many people in many organizations. NOAA’s Air Resources Laboratory, Office of Global Programs, and, more recently, NOAA’s Climate Observations and Services Program have provided primary funding for the network. NASA has supplemented SURFRAD with special funding for EOS validation. The accuracies and precision of SURFRAD measurements would not be possible without the generous contributions of DOE’s National Renewable Energy Laboratory who have impeccably calibrated all of SURFRAD’s shortwave instruments to world standards. Likewise, NOAA’s Central UV Calibration Facility provides the basis for world-class calibrations of the UVB instruments used in

the network. The Atmospheric Turbulence and Diffusion Division of NOAA's Air Resources Laboratory provides professional care to the network's wind monitors. Penn State, the USDA, the USGS, the Fort Peck Tribes, ARL's Special Operations and Research Division, and the Illinois State Water Survey provide telephone service, utilities, general maintenance, and expert troubleshooting at the stations they host. All of the

aforementioned services are provided at little or no cost to the program in the spirit of good science and high-quality measurements. NOAA's SURFRAD program also enjoys the close collaboration of Chuck Long of DOE's Atmospheric Radiation Measurements Program, John DeLuisi, and Ellsworth Dutton, whose work has generally improved the quality and usefulness of surface radiation measurements.

APPENDIX

Uncertainties in Diffuse Solar Corrections at the 95% Confidence Level for Each SURFRAD Station

Period	Pyranometer type	DpirNet value of inflection point (W m^{-2})	Uncertainty of clearer/dry data (W m^{-2})	Uncertainty of cloudy/wet data (W m^{-2})
Bondville				
27 Aug–1 Nov 1996	Spectrolab	–100	± 1.32	± 1.18
2 Nov 1996–21 May 1997	Spectrolab		Daily mean night diffuse signal used	
22 May–8 Jul 1997	Spectrolab	–90	± 0.70	± 0.74
9 Jul 1997–18 Jun 1998	Spectrolab	–100	± 1.07	± 1.09
19 Jun–17 Jul 1998	Spectrolab	–80	± 0.76	± 0.76
18 Jul 1998–19 Jul 1999	Spectrolab		Daily mean night diffuse signal used	
20 Jul 1999–19 Jun 2000	Spectrolab	–90	± 1.46	± 1.58
20 Jun 2000–20 May 2001	Spectrolab	–80	± 1.37	± 1.53
Fort Peck				
11 Oct 1996–23 Sep 1997	Spectrolab	–120	± 1.80	± 1.60
24 Sep–2 Nov 1997	Spectrolab	–100	± 2.02	± 2.32
3 Nov 1997–22 Aug 1998	Spectrolab		Daily mean night diffuse signal used	
23 Aug–22 Sep 1998	Spectrolab	–100	± 1.95	± 1.63
23 Sep 1998–13 Oct 1999	Spectrolab	–100	± 0.79	± 0.93
14 Oct 1999–7 Oct 2000	Spectrolab	–90	± 1.71	± 1.84
8 Oct 2000–5 Jul 2001	Spectrolab	–80	± 1.82	± 1.83
6 Jul –23 Jul 2001	Spectrolab		Station down due to lightning strike	
24 Jul–2 Oct 2001	Spectrolab	–90	± 2.07	± 1.98
Goodwin Creek				
11 Apr–13 Oct 1996	Spectrolab	–100	± 1.55	± 1.26
14 Oct 1996–9 Jul 1997	Spectrolab		Daily mean night diffuse signal used	
10 Jul 1997–1 Jun 1998	Spectrolab	–90	± 1.03	± 1.02
2 Jun 1998–17 Jan 1999	Spectrolab	–100	± 1.31	± 1.19
18 Jan–21 Apr 1999	Spectrolab		Daily mean night diffuse signal used	
22 Apr–6 May 1999	Spectrolab	–90	± 1.48	± 1.79
7 May–21 Jun 1999	Spectrolab		Daily mean night diffuse signal used	
22 Jun 1999–4 Apr 2000	Spectrolab	–80	± 1.15	± 1.12
5 Apr 2000–16 Apr 2001	Spectrolab	–100	± 1.22	± 1.40
Table Mountain				
19 Jun–13 Jul 1995	Eppley	–110	± 4.08	± 2.95
14 Jul–16 Jul 1995	Eppley		Daily mean night diffuse signal used	
17 Jul–8 Nov 1995	Spectrolab	–120	± 2.10	± 1.59
9 Nov 1995–17 Jan 1996	Spectrolab	–100	± 1.30	± 1.30
18 Jan–4 Mar 1996	Spectrolab		Daily mean night diffuse signal used	
5 Mar–25 Jul 1996	Spectrolab	–110	± 1.28	± 1.43
26 Jul 1996–7 Feb 1997	Spectrolab	–110	± 1.38	± 1.75
8 Feb–20 Jul 1997	Spectrolab	–150	± 1.72	± 1.94
21 Jul–26 Aug 1997	Spectrolab	–110	± 1.29	± 1.52
27 Aug 1997–1 Mar 1998	Spectrolab	–100	± 1.36	± 1.42
2 Mar–17 Aug 1998	Spectrolab	–110	± 1.51	± 1.63
18 Aug 1998–2 Sep 1999	Spectrolab	–100	± 1.58	± 1.94
3 Sep 1999–28 Aug 2000	Spectrolab	–110	± 1.55	± 1.82
29 Aug 2000–6 Sep 2001	Spectrolab	–100	± 1.88	± 2.18

(Continued)

Period	Pyranometer type	DpirNet value of inflection point (W m ⁻²)	Uncertainty of clearer/dry data (W m ⁻²)	Uncertainty of cloudy/wet data (W m ⁻²)
Desert Rock				
15 Mar 1998–22 May 1999	Spectrolab	–110	±1.67	±1.61
23 May–22 Jun 1999	Spectrolab	–110	±1.46	±1.21
23 Jun–10 Oct 1999	Spectrolab	–120	±1.52	±1.33
11–17 Oct 1999	Spectrolab		Daily mean night diffuse signal used	
18 Oct 1999–1 May 2000	Spectrolab	–120	±2.00	±1.69
2 May 2000–26 Mar 2001	Eppley	–100	±1.39	±1.58
Penn State				
29 Jun 1998–12 Aug 1999	Spectrolab	–100	±1.51	±1.38
13 Aug 1999–15 Jun 2000	Eppley	–90	±1.61	±2.29
16 Jun–10 Jul 2000	Eppley	–85	±2.85	±2.99
11 Jul 2000–28 Aug 2001	Spectrolab	–100	±1.70	±1.81

REFERENCES

- Albrecht, B., and S. K. Cox, 1977: Procedures for improving pyrometer performance. *J. Appl. Meteor.*, **16**, 188–197.
- Augustine, J. A., J. J. DeLuisi, and C. N. Long, 2000: SURFRAD—A national surface radiation budget network for atmospheric research. *Bull. Amer. Meteor. Soc.*, **81**, 2341–2357.
- , C. R. Cornwall, G. B. Hodges, C. N. Long, C. I. Medina, and J. J. DeLuisi, 2003: An automated method of MFRSR calibration for aerosol optical depth analysis with application to an Asian dust outbreak over the United States. *J. Appl. Meteor.*, **42**, 266–278.
- Cleveland, W. S., 1979: Robust locally weighted regression and smoothing scatterplots. *J. Amer. Stat. Assoc.*, **74**, 829–836.
- , and S. J. Devlin, 1988: Locally weighted regression: An approach to regression analysis by local fitting. *J. Amer. Stat. Assoc.*, **83**, 596–610.
- Committee on Global Climate Research, 1998: *Global Environmental Change: Research Pathways for the Next Decade, Overview*. National Academic Press, 82 pp.
- Dutton, E. G., J. J. Michalsky, T. Stoffel, B. W. Forgan, J. Hickey, D. W. Nelson, T. L. Alberta, and I. Reda, 2001: Measurement of broadband diffuse solar irradiance using current commercial instrumentation with a correction for thermal offset errors. *J. Atmos. Oceanic Technol.*, **18**, 297–314.
- Gulbrandsen, A., 1978: On the use of pyranometers in the study of spectral solar radiation and atmospheric aerosols. *J. Appl. Meteor.*, **17**, 899–904.
- Heim, R., 2001: New network to monitor climate change. *Eos, Trans. Amer. Geophys. Union*, **82**, 143.
- Jin, Y., C. B. Schaaf, C. E. Woodcock, F. Gao, X. Li, A. H. Strahler, W. Lucht, and S. Liang, 2003: Consistency of MODIS surface BRDF/Albedo retrievals: 2. Validation. *J. Geophys. Res.*, **108**, 4159, doi:10.1029/2002JD002804.
- Karl, T. P., P. Y. Groisman, R. W. Knight, and R. R. Heim Jr., 1993: Recent variations of snow cover and snowfall in North America and their relation to precipitation and temperature variations. *J. Climate*, **6**, 1327–1344.
- Lantz, K. O., P. Disterhoft, J. J. DeLuisi, E. Early, A. Thompson, D. Bigelow, and J. Slusser, 1999: Methodology for deriving clear-sky erythemal calibration factors for UV broadband radiometers of the U.S. Central UV Calibration Facility. *J. Atmos. Oceanic Technol.*, **16**, 1736–1752.
- Long, C. N., and T. P. Ackerman, 2000: Identification of clear skies from broadband pyranometer measurements and calculation of downwelling shortwave cloud effects. *J. Geophys. Res.*, **105**, 15 609–15 626.
- , —, and J. J. DeLuisi, 1999: Estimation of fractional sky cover from broadband SW radiometer measurements. *Proc. 10th Conf. on Atmospheric Radiation*, Madison, WI, Amer. Meteor. Soc., 383–386.
- Marty, C., and Coauthors, 2003: Downward longwave irradiance uncertainty under arctic atmospheres: Measurements and modeling. *J. Geophys. Res.*, **108**, 4358, doi:10.1029/2002JD002937.
- McArthur, L. J. B., 1998: Baseline Surface Radiation Network (BSRN) Operations Manual (Version 1.0). World Climate Research Programme, WMO Tech. Doc. 879, 69 pp.
- Michalsky, J. J., J. A. Schlemmer, W. E. Berkheiser, J. L. Berndt, L. C. Harrison, N. S. Laulainen, N. R. Larson, and J. C. Barnard, 2001: Multiyear measurements of aerosol optical depth in the Atmospheric Radiation Measurement and Quantitative Links programs. *J. Geophys. Res.*, **106** (D11), 12 099–12 107.
- Morcrette, J. J., 2002a: Assessment of the ECMWF model cloudiness and surface radiation fields at the ARM SGP site. *Mon. Wea. Rev.*, **130**, 257–277.
- , 2002b: The surface downward longwave radiation in the ECMWF forecast system. *J. Climate*, **15**, 1875–1892.
- Philipona, R., 2001: Sky-scanning radiometer for absolute measurements of atmospheric longwave radiation. *Appl. Opt.*, **40**, 2376–2383.
- , and Coauthors, 1998: The baseline surface radiation network pyrometer round-robin calibration experiment. *J. Atmos. Oceanic Technol.*, **15**, 687–696.
- , and Coauthors, 2001: Atmospheric longwave irradiance uncertainty: Pyrometers compared to an absolute sky-scanning radiometer, atmospheric emitted radiance interferometer, and radiative transfer model calculations. *J. Geophys. Res.*, **106** (D22), 28 129–28 141.

- Pinker, R. T., and Coauthors, 2003: Surface radiation budgets in support of the GEWEX Continental-Scale International Project (GCIP) and the GEWEX Americas Prediction Project (GAPP), including the North American Land Data Assimilation System (NLDAS) project. *J. Geophys. Res.*, **108**, 8844, doi:10.1029/2002JD003301.
- Shaw, G. E., 1983: Sun photometry. *Bull. Amer. Meteor. Soc.*, **64**, 4–10.
- Sun, D., and R. T. Pinker, 2003: Estimation of land surface temperature from a Geostationary Operational Environmental Satellite (GOES-8). *J. Geophys. Res.*, **108**, 4326, doi:10.1029/2002JD002422.
- Wolfe, D. E., and S. I. Gutman, 2000: Development of the NOAA/ERL Ground-Based GPS Water Vapor Demonstration Network: Design and Initial Results. *J. Atmos. Oceanic Technol.*, **17**, 426–440.